International Journal of Automotive Technology, Vol. 16, No. 4, pp. 669−683 (2015)
DOI 10.1007/s12239−015−0068−4

pISSN 1229−9138/ eISSN 1976−3832

CORNERING STIFFNESS AND SIDESLIP ANGLE ESTIMATION BASED ON SIMPLIFIED LATERAL DYNAMIC MODELS FOR FOUR-IN-WHEEL-MOTOR-DRIVEN ELECTRIC VEHICLES WITH LATERAL TIRE FORCE INFORMATION

Y. F. LIAN[1, 3], Y. ZHAO[1], L. L. HU[1] and Y. T. TIAN[1, 2]*

[1]College of Communication Engineering, Jilin University, Changchun 130025, China
[2]Key Laboratory of Bionics Engineering, Ministry of Education, Jilin University, Changchun 130025, China
[3]School of Electrical and Electronic Engineering, Changchun University of Technology, Changchun 130025, China

(Received 20 January 2014; Revised 24 October 2014; Accepted 18 November 2014)

ABSTRACT−The simplified lateral dynamic models of front and rear tires are proposed with lateral tire force information in this paper. The regression models of the recursive least squares (RLS) with forgetting factors and constraints are constructed based on simplified lateral dynamic models for estimating tire cornering stiffness. In addition, a nonlinear observer of sideslip angle is designed for four-in-wheel-motor-driven electric vehicles (FIWMD-EVs) with the estimated information on tire cornering stiffness. Sideslip angle can be estimated through a first-order Stirling's interpolation filter (DD1-filter) and a first-order low-pass filter. The reliability, feasibility, effectiveness, and practicality of simplified lateral dynamic models are verified by contrast simulation experiments. The simplified lateral dynamic models of front and rear tires are not influenced on the change of sideslip angle, nor influenced by each other. Moreover, it can result in improving computation speed that computational burden is reduced after simplifying lateral dynamic models. With the estimated information above mentioned, sideslip angle is also estimated well. The estimated information on tire cornering stiffness and sideslip angle is benefit to the design of lateral stability control system, which can make vehicle adapt to different road conditions and control the steering motion attitude of vehicle in future works.

KEY WORDS : Simplified lateral dynamic models, Lateral tire force information, Tire cornering stiffness estimation, Sideslip angle estimation

1. INTRODUCTION

Extensive investigations have shown that over 90% of road accidents occur as a result of driver errors: losing control of vehicle, exceeding speed limits, leaving the road at the high speed, etc (Aparicio *et al.*, 2005; Doumiati *et al.*, 2011; Shino *et al.*, 2014). Such accidents can be avoided by some vehicle control systems, especially active safety control system, such as adaptive cruise control (ACC), anti-lock braking systems (ABS), traction control (TC), electronic stability program (ESP), collision warning (CW), collision avoidance (CA) and four-wheel steering (4WS) (Rajamani, 2005; Jazar, 2008; Lian *et al.*, 2012). Some parameters' information on vehicle motion, such as sideslip angle, cornering stiffness, tire-road friction condition, vehicle velocity and so forth, is one of the most significant factors for active safety system, both for improving the handling and safety of vehicle and for achieving the intelligent vehicle initiative concept in the near future (Huh and Kim, 2001; Arndt *et al.*, 2004; Imsland *et al.*, 2006; Wenzel *et al.*, 2006; Cheli *et al.*, 2007; Han and Huh, 2011; Ko *et al.*, 2014). Some parameters can be available by inexpensive measurements in vehicle control systems, such as rotational velocity for each wheel measured by magnetic, acceleration measured by accelerometer, yaw rate measured by gyro meter, steering angle measured by an optical sensor and so forth. With the enhancing requirement unceasingly of people for active safety system, more parameters are required for research and design of vehicle control systems, such as sideslip angle (Geng *et al.*, 2007; Geng *et al.*, 2009), tire-road friction condition (Sado *et al.*, 1999) and so on. Although they can be also measured by instrumental sensors directly, it is not feasible to install these sensors in vehicles due to high cost and lack of reliability. Therefore, taking technical, physical, and economic reasons into account, appropriate indirect sensing methods are necessary to monitor lateral motion so that these limitations can be overcome. The control structure of lateral stability control system for FIWMD-EVs can be described in Figure 1. The driver's cornering intention can be chosen as the input of desired vehicle model, yaw rate

**Corresponding author.* e-mail: tianyt@jlu.edu.cn

and sideslip angle can be chosen as the responses of desired vehicle model. The yaw rate and sideslip angle of vehicle can be controlled in vehicle lateral motion as state variables to enhance vehicle handling performance and maintain stability. Besides yaw rate and sideslip angle, another parameter is required to provide the information on road condition to make vehicle adapt to different road conditions. Fortunately, road condition can be represented by tire cornering stiffness, the information on tire cornering stiffness can be employed to design adaptive controller of vehicle lateral motion. Therefore, yaw rate, sideslip angle, and tire cornering stiffness are needed in controller design of vehicle lateral motion. Yaw rate can be measured directly mentioned above, so there are two parameters to need estimating, namely sideslip angle and tire cornering stiffness shown by grey segment in Figure 1. The estimation motheds of sideslip angle and tire cornering stiffness can be studied in this work.

For sideslip angle, it can be used in design of lateral stability control system. For example, D.Lechner *et al.* used the information on yaw rate, lateral acceleration, and vehicle velocity to estimate sideslip angle (Lechner, 2008), and calculating sideslip angle is easy to be obtained from sideslip rate integration. Some observer-direct integration methods are presented to estimate sideslip angle by Nishio *et al.* (2001) and Piyabongkarn *et al.* (2009). Baffet *et al.* (2006) take a nonlinear bicycle model into account for estimating sideslip angle. A nonlinear adaptive observer with an added algorithm for sideslip angle is designed by Grip *et al.* (2009). There are some errors and uncertainty in computational process or estimation process for these methods.

For tire cornering stiffness, it can be changed in terms of the tire slip angle and road friction (Fujimoto *et al.*, 2005). The information on tire cornering stiffness is conducive to design vehicle controller to adapt to different road conditions. However, it is hard to be available resulting from the nonlinear characteristics of tire model principally. Therefore, a number of estimation methods have been proposed for obtaining the information on tire cornering stiffness (Sierra *et al.*, 2006). The estimation of tire cornering stiffness is contributing significantly to not only estimate sideslip angle (Cheli *et al.*, 2007), but also improve active steering control system (Sienel, 1997). They are divided into two groups mainly; one group is simultaneous estimation of sideslip angle and tire cornering stiffness. For example, combining with yaw moment observer, Fujimoto *et al.* (2006) proposed a simultaneous estimation for sideslip angle and tire cornering stiffness. GPS antenna is used to construct the simultaneous estimator by Anderson and Bevly (2005). A sliding mode estimator for sideslip angle and tire cornering stiffness is proposed by Baffet *et al.* (2007). These methods make estimator burden in computational process resulting from complication. Another group is the estimation of tire cornering stiffness without sideslip angle (Nguyen *et al.*, 2011). A new sensor, which is used in vehicle, is developed to measure tire lateral force by Leeuween *et al*. (2007). It becomes a new effective solution for vehicle state estimation (Nguyen *et al.*, 2011; Nam *et al.*, 2012), and has been developed by both academic research and industry circles (Holweg, 2008; Tunonen, 2008; Nguyen *et al.*, 2011). In this work, the methods, which are used by the second group, are also employed for obtaining the information on tire cornering stiffness. The simplified lateral dynamic models of front and rear tires are deduced with lateral force information from lateral force sensors for constructing regression model of RLS with forgetting factors and constraints. In addition to this, several monitoring systems are designed based on 2-degree-of-freedom (2-DOF) models of vehicle or 3-degree-of-freedom (3-DOF) model of vehicle (Han and Huh, 2011). 2-DOF model of vehicle is used widely for not only designing vehicle control system, but also describing the driver's familiar characteristics under normal driving conditions (Geng *et al.*, 2009). Therefore, the new simplified lateral dynamic models are derived from the 2-DOF model of vehicle. The estimation models are derived

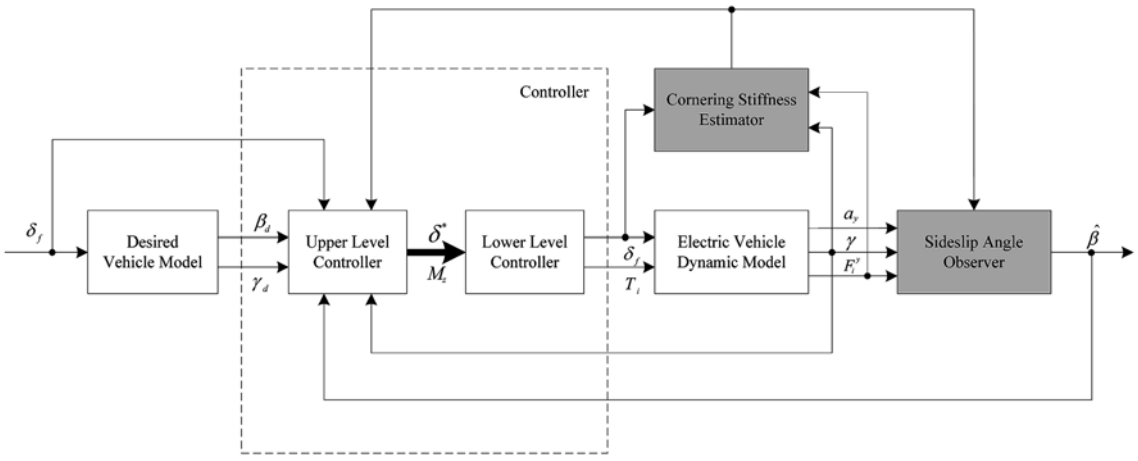

Figure 1. Control structure of lateral stability control system.

from new simplified lateral dynamic models, which are much simpler than before simplifying (Nguyen *et al.*, 2011). The feasibility, effectiveness, and practicality of the simplified lateral dynamic models are verified by contrast simulation experiments. The simplified lateral dynamic models of front and rear tires, which are not influenced on the change of sideslip angle, can be used to estimate tire cornering stiffness with lateral tire force information to avoid complicated coupled structures. Consequently, they can simplify the structure of estimation models, alleviate computational burden and improve computation speed. Besides that, with the information on tire cornering stiffness, a nonlinear observer of sideslip angle is designed for FIWMD-EVs, and sideslip angle is estimated well combining a DD1-filter with a first-order low-pass filter. In this work, tire cornering stiffness and the sideslip angle of vehicle can be chosen to be estimated for two reasons, one is that the steering motion controller of vehicle can be designed to adapt to different road conditions with the information on tire cornering stiffness; another is that the steering motion attitude of vehicle can be controlled with the information on sideslip angle. Therefore, tire cornering stiffness and sideslip angle are worthy of being studied.

The remaining paper is organized as follows. In Section 2, vehicle dynamic model is described, and the state equations of vehicle are given with small angle approximation. In Section 3, the basic of lateral tire force is introduced, and simplified lateral dynamic models are derived. Estimation algorithm of tire cornering stiffness is presented in this section. In Section 4, dynamic longitudinal tire force models and dynamic lateral tire force models are described. Tire force distribution problem for FIWMD-EVs is discussed. In Section 5, a nonlinear observer of sideslip angle is designed for FIWMD-EVs, and the DD1-filter is introduced in this section. Simulation study on the performance of the estimation algorithm of tire cornering stiffness based on simplified lateral dynamic models and sideslip angle based on a nonlinear observer for FIWMD-EVs is conducted. Simulation results are presented and discussed in Section 6. Finally, a conclusion regarding research and future works is made in Section 7.

2. VEHICLE DYNAMIC MODEL

A yaw plane model is introduced to describe the lateral motion of FIWMD-EVs with 2-DOF vehicle motion in the longitudinal and lateral planes. The yaw angle around the vertical axis is taken as positive in the anti-clockwise direction. Vehicle longitudinal direction is represented with x, and vehicle lateral direction is represented with y. The origin of coordinate system is at the vehicle center of gravity (CG) (Abe and Manning, 2009). The equations of motion for the lateral dynamics of the four-wheel model, as shown in Figure 2 (a), are given by,

$$mv_x\left(\frac{d\beta}{dt}+\gamma\right) = (F_{fl}^x+F_{fr}^x)\sin\delta_f+(F_{fl}^y+F_{fr}^y)\cos\delta_f+F_{rl}^y+F_{rr}^y \quad (1)$$

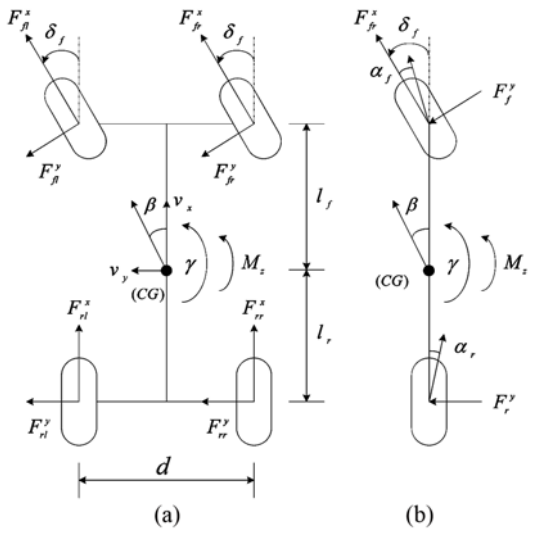

Figure 2. Planar vehicle models: (a) Four-wheel model; (b) Two-wheel model.

$$I_z\frac{d\gamma}{dt} = l_f[(F_{fl}^x+F_{fr}^x)\sin\delta_f+(F_{fl}^y+F_{fr}^y)cos\,\delta_f] - l_r(F_{rl}^y+F_{rr}^y)+M_z \quad (2)$$

where, m is total mass of vehicle; v_x is longitudinal velocity at CG; β is vehicle sideslip angle at CG; γ is yaw rate; F_{fl}^x is longitudinal force acting on the front-left tire; F_{fr}^x is longitudinal force acting on the front-right tire; F_{rl}^x is longitudinal force acting on the rear-left tire; F_{rr}^x is longitudinal force acting on the rear-right tire; F_{fl}^y is lateral force acting on the front-left tire; F_{fr}^y is lateral force acting on the front-right tire; F_{rl}^y is lateral force acting on the rear-left tire; F_{rr}^y is lateral force acting on the rear-right tire; δ_f is front steering angle; I_z is yaw moment of inertia; l_f is distance from CG to front axle; l_r is distance from CG to rear axle, and $l = l_f + l_r$; M_z is yaw moment generated by motor torque difference between each wheel, which is an additional input variable. It can be calculated as follows:

$$M_z = \frac{d}{2}(F_{rr}^x-F_{rl}^x)+\frac{d}{2}(F_{fr}^x-F_{fl}^x)\cos\delta_f \quad (3)$$

where, d is track width, the front and rear track widths are assumed to be equal.

For design simplicity, assuming that the driving conditions between front and rear wheels are identical and the driving conditions between left and right wheels are also identical, as shown in Figure 2 (b), the equations of motion for the lateral dynamics of the two-wheel model is given by,

$$mv_x\left(\frac{d\beta}{dt}+\gamma\right) = F_f^y\cos\delta_f+F_r^y \quad (4)$$

$$I_z\frac{d\gamma}{dt} = l_f F_f^y\cos\delta_f - l_r\,F_r^y+M_z \quad (5)$$

For small tire slip angles, lateral tire forces can be

linearly approximated as follows:

$$F_f^y = -2C_f\left(\beta + \frac{\gamma l_f}{v_x} - \delta_f\right) \tag{6}$$

$$F_r^y = -2C_r\left(\beta - \frac{\gamma l_r}{v_x}\right) \tag{7}$$

where, C_f is the cornering stiffness of front tires; C_r is the cornering stiffness of rear tires.

With small angle approximation, let sideslip angle and yaw rate represent the system state variables. Assuming that δ_f is relatively small for high speeds and substituting (6) and (7) into (4) and (5), the state equations of vehicle are obtained as follows:

$$\begin{cases} \dot{x} = \mathbf{A}x + \mathbf{B}u \\ y = \mathbf{C}x \end{cases} \tag{8}$$

where, $x = \begin{bmatrix}\beta & \gamma\end{bmatrix}^T$; $u = \begin{bmatrix}\delta_f & M_z\end{bmatrix}^T$; $y = \gamma$;

$$\mathbf{A} = \begin{bmatrix} \dfrac{-2(C_f + C_r)}{mv_x} & \dfrac{-2(l_f C_f - l_r C_r)}{mv_x^2} - 1 \\ \dfrac{-2(l_f C_f - l_r C_r)}{I_z} & \dfrac{-2(l_f^2 C_f + l_r^2 C_r)}{I_z v_x} \end{bmatrix};$$

$$\mathbf{B} = \begin{bmatrix} \dfrac{2C_f}{mv_x} & 0 \\ \dfrac{2l_f C_f}{I_z} & \dfrac{1}{I_z} \end{bmatrix}; \quad \mathbf{C} = \begin{bmatrix}0 & 1\end{bmatrix}.$$

As seen in (8), there are two state variables named sideslip angle and yaw rate, which can be controlled in vehicle lateral motion. Taking technical, physical, and economic reasons into account, sideslip angle is usually estimated instead of measuring directly. In lateral motion, the attitude of vehicle can be influenced on different road conditions. Fortunately, road conditions can be represented by tire cornering stiffness correspondingly. Therefore, tire cornering stiffness can be chosen to be estimated for obtaining the information on different road conditions.

In this work, tire cornering stiffness is estimated without the information on sideslip angle, and a nonlinear observer of sideslip angle is designed with the estimated information on cornering stiffness of front and rear tires. Therefore, the derivation process of tire cornering stiffness estimation is stated first, and the design process of sideslip angle estimation is stated later.

3. CORNERING STIFFNESS ESTIMATION

3.1. Lateral Dynamic Models Simplifying

Since the main nonlinearity in models comes from tires, tire cornering stiffness can play an important role in the formulation of models used in the estimation. For different road conditions, tire cornering stiffness can change correspondingly. Therefore, tire cornering stiffness, which can be estimated, is used to represent road condition correspondingly.

Combining (6) with (7), sideslip angle is eliminated as a variable as follows:

$$F_f^y = \frac{C_f}{C_r}F_r^y + 2C_f\left(\delta_f - \frac{l\gamma}{v_x}\right) \tag{9}$$

As seen in Figure 2 (a), the heading direction of the front wheels has an angular displacement of δ_f with respect to the vehicle longitudinal direction. The heading direction of the rear wheels is the same as the vehicle longitudinal direction. A FIWMD-EV, which has battery packs under the floor and driving motors attached in wheels, is taken into account and can lower the CG of vehicle. This provides less weight transfer and thereby improves driving stability. From these features, variations in the front-left and front-right tire cornering stiffness can be not taken into account (Nam *et al.*, 2012). It is assumed that tire cornering stiffness of the left and right tires are the same. Therefore, lateral forces acting on the front tires are given as follows:

$$F_{fl}^y = -C_f\left(\frac{v_x\beta + l_f\gamma}{v_x - \frac{d}{2}\gamma} - \delta_f\right) \tag{10}$$

$$F_{fr}^y = -C_f\left(\frac{v_x\beta + l_f\gamma}{v_x + \frac{d}{2}\gamma} - \delta_f\right) \tag{11}$$

Combining (10) with (11), lateral forces acting on the front tires can be also expressed as follows:

$$\left(v_x + \frac{d}{2}\gamma\right)F_{fr}^y - \left(v_x - \frac{d}{2}\gamma\right)F_{fl}^y = d\gamma\delta_f C_f \tag{12}$$

Therefore, the regression models of tire cornering stiffness estimation can be obtained based on (9) and (12) (Tunonen, 2008; Nguyen *et al.*, 2011). Although tire cornering stiffness can be estimated without the information on sideslip angle of vehicle, the estimation effectiveness of cornering stiffness of front and rear tires can be influenced by each other, and matrix operations are required for estimating tire cornering stiffness based on (9) and (12), which can increase the computational burden and influence the computation speed of estimator. For this problem, the lateral dynamic models need simplifying to reduce the computational burden and improve the computation speed of estimator without affecting the accuracy of the premise.

Assuming that lateral force acting on the front-left tire and front-right tire are identical, namely, $F_{fl}^y = F_{fr}^y = \frac{1}{2}F_f^y$. Combining with (12), lateral forces acting on the front tires can be simplified as follows:

$$F_f^y = 2C_f\delta_f \tag{13}$$

Substituting (13) into (9), lateral forces acting on the rear tires can be simplified as follows:

$$F_r^y = \frac{2lC_r}{v_x}\gamma \tag{14}$$

As seen in (13) and (14), without the information on

sideslip angle, the cornering stiffness of front and rear tires can be estimated. Meanwhile, no interactive influences exist in estimating process. Furthermore, the regression models of tire cornering stiffness estimation based on (13) and (14), which are reduced greatly to avoid complicated coupled structures, are much simpler than that based on (9) and (12).

3.2. Recursive Least Squares (RLS) Algorithm

The simplified lateral dynamic models described in the previous section can be formulated in a parameter identification form as,

$$y(t) = \varphi^T(t)\theta(t) + e(t) \tag{15}$$

where, $\theta(t)$ is the vector of estimated parameters, $\varphi(t)$ is the regression vector, $e(t)$ is the identification error between measured $y(t)$ and estimated value $\varphi^T(t)\theta(t)$. Therefore, from (9) and (12), the regression models of tire cornering stiffness estimation can be defined as follows:

$$\begin{cases} y_{(9),(12)}(t) = \begin{bmatrix} F_f^y \\ \left(v_x + \frac{d}{2}\gamma\right)F_{fr}^y - \left(v_x - \frac{d}{2}\gamma\right)F_{fl}^y \end{bmatrix} \\ \varphi_{(9),(12)}^T(t) = \begin{bmatrix} F_r^y & 2\left(\delta_f - \frac{l\gamma}{v_x}\right) \\ 0 & d\gamma\delta_f \end{bmatrix} \\ \theta_{(9),(12)}(t) = \begin{bmatrix} \frac{C_f}{C_r} & C_f \end{bmatrix}^T \end{cases} \tag{16}$$

From (13) and (14), the regression models of tire cornering stiffness estimation can be defined as follows:

$$\begin{cases} y_{(13),(14)}(t) = \begin{bmatrix} F_f^y F_r^y \end{bmatrix}^T \\ \varphi_{(13),(14)}^T(t) = \begin{bmatrix} 2\delta_f & 0 \\ 0 & \frac{2l\gamma}{v_x} \end{bmatrix} \\ \theta_{(13),(14)}(t) = \begin{bmatrix} C_f & C_r \end{bmatrix}^T \end{cases} \tag{17}$$

RLS algorithm is used to iteratively update the unknown parameter vector, $\theta(t)$, at each sampling time, using the past input and output data contained within the regression vector, $\varphi(t)$. RLS algorithm updates the unknown parameters so as to minimize the sum of the square of the modeling errors. The procedure of RLS algorithm at each step t is as follows:

Step 1: Measure the system output, $y(t)$, and calculate the regression vector, $\varphi(t)$.

Step 2: Calculate the identification error, $e(t)$.

$$e(t) = y(t) - \varphi^T(t)\theta(t-1) \tag{18}$$

Step 3: Calculate the update gain vector, $K(t)$, and covariance matrix, $P(t)$.

$$K(t) = \frac{P(t-1)\varphi(t)}{\lambda + \varphi^T(t)P(t-1)\varphi(t)} \tag{19}$$

$$P(t) = \frac{1}{\lambda}\left[P(t-1) - \frac{P(t-1)\varphi(t)\varphi^T(t)P(t-1)}{\lambda + \varphi^T(t)P(t-1)\varphi(t)}\right] \tag{20}$$

Step 4: Update the parameter estimate vector, $\theta(t)$.

$$\theta(t) = \theta(t-1) + K(t)e(t) \tag{21}$$

The parameter, λ, in the aforementioned equations, is called the forgetting factor. It is used to effectively reduce the influence of old data which may no longer be relevant to the model. This allows the parameter estimates to track changes in the process quickly. A typical value for λ is in the interval (0.9, 1) (Rajamani *et al.*, 2012). According to the estimating process of tire cornering stiffness, RLS can be achieved with some constraints, which can be discussed in section 6.

4. TIRE DYNAMIC MODEL AND FORCE DISTRIBUTION

A tire can be considered as a force and moment generators. These forces and moments from road act on each tire of vehicle and highly influence the dynamics of vehicle. To designing a sideslip angle observer for FIWMD-EVs, the information on the longitudinal forces and lateral forces of front and rear tires is required, and the dynamic model of tire is also needed. Therefore, the dynamic longitudinal tire force model, the dynamic lateral tire force model, and the tire forces distribution constraints can be discussed in this section.

4.1. Dynamic Longitudinal Tire Force Model

As seen in (3), yaw moment M_z can be obtained with longitudinal tire forces. An observer is designed based on wheel rotational motion to obtain the information on longitudinal tire forces (Sado *et al.*, 1999). Transfer function of this observer, which is also used to estimate longitudinal tire forces, is given as follows (Nam *et al.*, 2012):

$$\widehat{F}_i^x(s) = \frac{\omega_d}{s + \omega_d}\left(\frac{T_i^m - I_\omega \omega_i s}{r}\right) \tag{22}$$

where, i is corresponding to the front-left, front-right, rear-left, and rear-right tires (=*fl*, *fr*, *rl*, *rr*). T_i^m is in-wheel motor torque which is measured from the motor current; I_w is wheel angular moment of inertia; r is tire radius; ω_i is angular velocity of wheel; ω_d is a cutoff frequency of the applied low-pass filter. Therefore, this observer can be employed to provide longitudinal tire force information to design sideslip angle observer in this work, which is designed in the section 5.

4.2. Dynamic Lateral Tire Force Model

Although there are many tire models which have been developed, taking the transient behavior of tire into account

and constructing a new nonlinear observer of sideslip angle for estimating sideslip angle of vehicle, a typical dynamic model that can be used for lateral tire force dynamics is first order and represented by (Rajamani, 2005),

$$\tau_{lag}\dot{F}_{y\_lag} + F_{y\_lag} = F_y \tag{23}$$

where, F_y is tire lateral force; F_{y_lag} is dynamic or lagged lateral force; time constant τ_{lag} is the relaxation time constant.

Substituting (6) and (7) into (23), the dynamic lateral tire force models for front and rear tires, which can be employed to construct sideslip angle observer of vehicle, are obtained as follows:

$$\begin{cases} \dot{F}_f^y = -\dfrac{1}{\tau_f}F_f^y - \dfrac{2C_f}{\tau_f}\beta - \dfrac{2C_f\, l_f}{\tau_f v_x}\gamma + \dfrac{2C_f}{\tau_f}\delta_f \\ \dot{F}_r^y = -\dfrac{1}{\tau_r}F_r^y - \dfrac{2C_r}{\tau_r}\beta + \dfrac{2C_r l_r}{\tau_r v_x}\gamma \end{cases} \tag{24}$$

4.3. Tire Forces Distribution

According to (8), the information on yaw moment, which is calculated with the longitudinal forces of four tires, is required. Therefore, the distribution problem on tire forces is necessary to be investigated in not only lateral stability control of vehicle, but also sideslip angle estimation of vehicle. Tire forces distribution is based on the classical Law of Friction mainly for the longitudinal and lateral forces of four tires. In addition, some constraints for tire forces distribution are taken into account. There are several different types of constraints for tire forces distribution. As seen in Figure 3, the tire's limits are determined by vertical load, road conditions and tire characteristics in Figure 3 (a), the lateral actuator limits are determined by steering, the longitudinal actuator limits are determined by the availability of braking and traction forces in Figure 3 (b) and Figure 3 (c), and the resulting limits can be shown in Figure 3 (d) (Fredriksson *et al.*, 2004). The constraints can be used to obtain the appropriate information on longitudinal and lateral tire forces to participate in estimating parameter and controlling attitude of vehicle in steering motion.

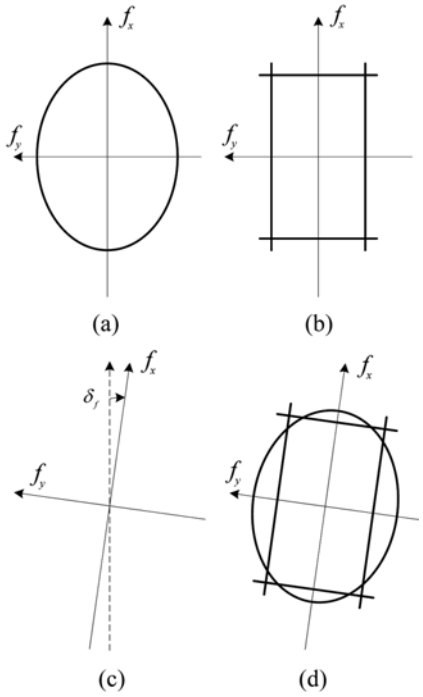

Figure 3. Constraints for a wheel unit: (a) Tire limits; (b) Actuator limits; (c) Wheel position; (d) Resulting limits.

Based on the analysis mentioned above, the distribution problem can be stated as,

$$\begin{cases} (F_{fl}^x)^2 + (F_{fl}^y)^2 \le (\mu_{fl}F_{fl}^z)^2 \\ (F_{fr}^x)^2 + (F_{fr}^y)^2 \le (\mu_{fr}F_{fr}^z)^2 \\ (F_{rl}^x)^2 + (F_{rl}^y)^2 \le (\mu_{rl}F_{rl}^z)^2 \\ (F_{rr}^x)^2 + (F_{rr}^y)^2 \le (\mu_{rr}F_{rr}^z)^2 \\ F_{fl}^x + F_{fr}^x + F_{rl}^x + F_{rr}^x > F_{aero} + R_f + F_{ace} + F_i \\ M_z + (F_{fl}^y + F_{fr}^y)l_f = (F_{rl}^y + F_{rr}^y)l_r \end{cases} \tag{25}$$

where, F_{aero} is the equivalent longitudinal aerodynamic drag force; R_f is the force due to rolling resistance; F_{acc} is the inertia force due to acceleration; F_i is the force due to gradient resistance; μ is friction coefficient for each tire. Therefore, the longitudinal and lateral tire forces can be all constrained by (25) to obtain the appropriate information on tire forces.

5. SIDESLIP ANGLE ESTIMATION

5.1. Design of Sideslip Angle Observer

A sideslip angle observer is designed, which is based on 2-DOF model of vehicle and dynamic lateral tire models. In order to make sideslip angle estimator adapt to different road conditions, tire cornering stiffness are considered in the design of nonlinear observer of sideslip angle. Therefore, the information on tire cornering stiffness estimated with simplified lateral dynamic models is used as a measurable state variable for nonlinear state equations in this sideslip angle observer. Taking FIWMD-EVs into account and combining (3) with tire forces distribution, the nonlinear state space equations of sideslip angle for FIWMD-EVs are expressed as follows:

$$\begin{cases} \dot{x}(t) = f(x(t), u(t)) + v(t) \\ y(t) = g(x(t)) + w(t) \end{cases} \tag{26}$$

where, the state vector is composed of the vehicle sideslip angle, yaw rate, front lateral tire force, rear lateral tire force, front tire cornering stiffness, and rear tire cornering stiffness,

$$x = [\beta, \gamma, F_f^y, F_r^y, C_f, C_r]^T = [x_1, x_2, x_3, x_4, x_5, x_6]^T \tag{27}$$

The measurement vector is composed of the yaw rate,

front lateral tire force, rear lateral tire force, front tire cornering stiffness, and rear tire cornering stiffness. The information on lateral tire forces from lateral force sensor is an effective solution and good for the state estimation of vehicles (Leeuween and Zuurbier, 2007),

$$y = [\gamma, F_f^y, F_r^y, C_f, C_r]^T = [y_1, y_2, y_3, y_4, y_5]^T \tag{28}$$

The input vector is composed of the front steering angle, front left driving force, front right driving force, rear left driving force, and rear right driving force,

$$u = [\delta_f, F_{fl}^x, F_{fr}^x, F_{rl}^x, F_{rr}^x]^T = [u_1, u_2, u_3, u_4, u_5]^T \tag{29}$$

The process and measurement noise vector are assumed to be of zero mean, white, and uncorrelated. Assuming that front tire cornering stiffness and rear tire cornering stiffness are invariant in the whole steering motion, namely,

$$\begin{cases} \dot{C}_f = 0 \\ \dot{C}_r = 0 \end{cases} \tag{30}$$

Combining (3) ~ (5) with (24) and (30), and considering tire dynamic model and forces distribution, the nonlinear state evolution function $f(x(t), u(t))$ and observation function $g(x(t))$ are expressed in (31) and (32), repectively. As seen in (31), front left driving force, front right driving force, rear left driving force, and rear right driving force are used to construct the input vector in the lateral motion for FIWMD-EVs. They can be obtained by the observer of tire longitudinal force, combining the constraints of a wheel unit mentioned above. Front lateral tire force, rear lateral tire force can be obtained directly from lateral force sensors.

$$\begin{cases} f_1(x,u) = -x_2 + \dfrac{x_3 \cos u_1}{m v_x} + \dfrac{x_4}{m v_x} \\ f_2(x,u) = \dfrac{l_f x_3 \cos u_1}{I_z} - \dfrac{l_r x_4}{I_z} \\ \qquad + \dfrac{d(u_5 - u_4 + u_3 \cos u_1 - u_2 \cos u_1)}{2I_z} \\ f_3(x,u) = -\dfrac{2x_1 x_5}{\tau_f} - \dfrac{2l_f x_2 x_5}{v_x \tau_f} - \dfrac{x_3}{\tau_f} + \dfrac{2x_5 u_1}{\tau_f} \\ f_4(x,u) = -\dfrac{2x_1 x_6}{\tau_r} + \dfrac{2l_r x_2 x_6}{v_x \tau_r} - \dfrac{x_4}{\tau_r} \\ f_5(x,u) = 0 \\ f_6(x,u) = 0 \end{cases} \tag{31}$$

$$\begin{cases} g_1(x) = x_2 \\ g_2(x) = x_3 \\ g_3(x) = x_4 \\ g_4(x) = x_5 \\ g_5(x) = x_6 \end{cases} \tag{32}$$

Based on aforementioned nonlinear dynamics, (26) is discretized as follows:

$$\begin{cases} x_{k+1} = f(x_k, u_k) + v_k \\ y_k = g(x_k) + w_k \end{cases} \tag{33}$$

5.2. State Estimation for Nonlinear System

According to the designed nonlinear observer of sideslip angle, a first-order extended Kalman filter (EKF) was used as the estimation algorithm of sideslip angle (Nam *et al.*, 2012). The EKF is based on first-order Taylor approximations of state transition and observation equations about the estimated state trajectory. However, the Taylor linearization provides an insufficiently accurate representation in many cases, and significant bias, or even convergence problems, are commonly encountered due to the overly crude approximation. A state estimator for nonlinear systems that is based on first-order polynomial approximations of the nonlinear mappings (Norgaard *et al.*, 2000) is applied in this paper. This filter is implemented easily without linearization of nonlinear system with Taylor's formula, therefore, the approximations obtained with Taylor's formula are avoided and the computational burden is reduced. The filter is used easily with the information on initialization of parameters and variances. The approximations are derived by using a multidimensional extension of Stirling's interpolation formula. This estimation algorithm of polynomial approximations called the first-order Stirling's interpolation filter (DD1-filter) is based on first-order approximations, which is described as follows (Norgaard *et al.*, 2000).

With the conditional expectations, the state estimate of (26) can be determined as follows:

$$\hat{x}_k = \bar{x}_k + K_k[y_k - \bar{y}_k] \tag{34}$$

where,

$$K_k = P_{xy}(k) P_y^{-1}(k), \tag{35}$$

$$\bar{x}_k = E[x_k | Y^{k-1}], \tag{36}$$

$$\bar{y}_k = E[y_k | Y^{k-1}], \tag{37}$$

$$P_{xy}(k) = E[(x_k - \bar{x}_k)(y_k - \bar{y}_k)^T | Y^{k-1}], \tag{38}$$

$$P_y(k) = E[(y_k - \bar{y}_k)(y_k - \bar{y}_k)^T | Y^{k-1}], \tag{39}$$

The corresponding update of the covariance matrix is

$$\begin{aligned} \hat{P}(k) &= E[(x_k - \hat{x}_k)(x_k - \hat{x}_k)^T | Y^k] \\ &= \bar{P}(k) - K_k P_y(k) K_k^T \end{aligned} \tag{40}$$

where, Y^{k-1} is a matrix containing the past measurements, $Y^{k-1} = [y_0, y_1, \ldots, y_{k-1}]^T$, and $Y^k = [y_0, y_1, \ldots, y_k]^T$.

5.3. DD1 Filter

The four square Cholesky factorizations is shown as follows:

$$Q = S_v S_v^T,\ R = S_w S_w^T, \bar{P} = \bar{S}_x \bar{S}_x^T, \hat{P} = \hat{S}_x \hat{S}_x^T \tag{41}$$

The a priori update of state estimate and covariance matrix for the state estimation error are given by,

$$\bar{x}_{k+1} \approx f(\hat{x}_k, u_k) + \bar{v}_k \tag{42}$$

$$\begin{aligned} \bar{P}(k+1) &= \bar{S}_x(k+1)\bar{S}_x^T(k+1) \\ &= [S_{x\hat{x}}(k)\ S_{xv}(k)][S_{x\hat{x}}(k)\ S_{xv}(k)]^T \end{aligned} \tag{43}$$

where, $S_{x\hat{x}}(k)$ and $S_{xv}(k)$ are divided differences,

$$\begin{aligned} S_{x\hat{x}}(k) &= \{S_{x\hat{x}}(k)_{(i,j)}\} \\ &= \{(f_i(\hat{x}_k + h\hat{s}_{x,j}, u_k) + \bar{v}_k \\ &- f_i(\hat{x}_k - h\hat{s}_{x,j}, u_k) - \bar{v}_k)/2h\} \end{aligned} \tag{44}$$

$$\begin{aligned} S_{xv}(k) &= \{S_{xv}(k)_{(i,j)}\} \\ &= \{(f_i(\hat{x}_k, u_k) + (\bar{v}_k + hs_{v,j}) \\ &- f_i(\hat{x}_k, u_k) - (\bar{v}_k - hs_{v,j}))/2h\} \end{aligned} \tag{45}$$

where, h denotes a selected interval length.

The a priori estimate of output and covariance matrix for the output estimation error are given by,

$$\bar{y}_k = g(\bar{x}_k) + \bar{w}_k \tag{46}$$

$$\begin{aligned} P_y(k) &= S_y(k)S_y^T(k) \\ &= [S_{y\bar{x}}(k) \quad S_{yw}(k)][S_{y\bar{x}}(k) \quad S_{yw}(k)]^T \end{aligned} \tag{47}$$

where, $S_{y\bar{x}}(k)$ and $S_{yw}(k)$ are divided differences,

$$\begin{aligned} S_{y\bar{x}}(k) &= \{S_{y\bar{x}}(k)_{(i,j)}\} \\ &= \{(g_i(\bar{x}_k + h\bar{s}_{x,j}) - g_i(\hat{x}_k - h\bar{s}_{x,j}))/2h\} \end{aligned} \tag{48}$$

$$\begin{aligned} S_{yw}(k) &= \{S_{yw}(k)_{(i,j)}\} \\ &= \{(g_i(\bar{x}_k) + (\bar{w}_k + hs_{w,j}) \\ &- g_i(\bar{x}_k) - (\bar{w}_k - hs_{w,j}))/2h\} \end{aligned} \tag{49}$$

The cross-covariance of state and output estimation error is obtained as follows:

$$P_{xy}(k) = \bar{S}_x(k)(S_{y\bar{x}}(k))^T \tag{50}$$

The recursive procedure of the DD1 algorithm at each step k is as follows:

Step 1: Calculate divided differences $S_{x\hat{x}}(k)$ and $S_{xv}(k)$ with (44) and (45) to obtain covariance matrix for the state estimation error $P(k+1)$ and $\bar{S}_x(k+1)$ with (43).

Step 2: Calculate divided differences, $S_{y\bar{x}}(k+1)$ and $S_{yw}(k+1)$ with (48) and (49) to obtain output covariance $S_y(k+1)$, covariance matrix for the output estimation error $P_y(k+1)$ and cross-covariance $P_{xy}(k+1)$.

Step 3: Calculate Kalman gain K_{k+1} with (35).

Step 4: Calculate a posteriori states $\hat{x}_{k+1}$ with (34).

Step 5: Covariance matrix update $\hat{P}(k+1)$ with (43).

6. SIMULATION RESULTS AND ANALYSIS

A case of simulation is conducted to verify the feasibility, effectiveness and practicality of estimation algorithm based on simplified lateral dynamic models for estimating tire cornering stiffness and sideslip angle. The electric vehicle specifications used in simulations are listed in Table 1. For simulation study, some simulation data are derived from simulation software CarSim 8.02, such as the formation on lateral motion trajectory, front steering angle, and lateral forces of front and rear tires, yaw rate. They can be measured by accelerometer, optical sensor, lateral tire force sensor, and gyro meter in practice, correspondingly. The data mentioned above can be used to estimate tire cornering stiffness and sideslip angle as given data. Moreover, it is assumed that the given data can be available after data processing for simulation requirement. According to the simplified lateral dynamic model, (13) can be used for estimating cornering stiffness without the information on cornering stiffness of rear tire, and (14) can be used for estimating cornering stiffness without the information on cornering stiffness of front tire. Therefore, the cornering stiffness of front and rear tires can be decoupled each other.

In addition, accurate parameter estimation depends on the qualities of the estimator input signal, such as the steering angle, yaw rate, and lateral tire forces. In other words, they are very small when the vehicle is driving straight; the experimental data are around the zero, where the estimated parameter will be stochastically uncertain. Therefore, to ensure the good estimator performance for FIWMD-EVs, the estimated tire cornering stiffness can be not updated when the absolute values of the steering angle and yaw rate are less than certain small values (Nam *et al.*, 2012). However, there constraints are just not enough for obtaining the good estimation performance of tire cornering stiffness estimator. The input signal mentioned above may be very small during the steering motion of vehicle, and these signals around the zero can produce large estimation error resulting in the poor estimation

Table 1. Specifications of electric vehicle.

Type	Definition	Value
Vehicle parameters	Mass (kg)	1159
	Gravity acceleration (m/s^2)	9.8
	Distance between center of mass and front shaft (m)	1.04
	Distance between center of mass and rear shaft (m)	1.56
	Height of center of mass (m)	0.5
	Track width (m)	1.5

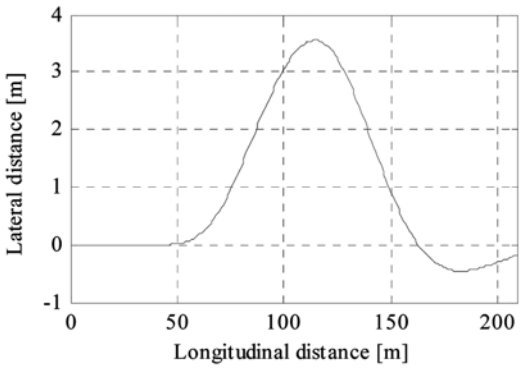

Figure 4. Lateral motion trajectory.

performance of tire cornering stiffness estimator. Therefore, besides the certain small values mentioned above, another constraint can be taken into account for ensuring the good estimator performance for FIWMD-EVs. The estimated tire cornering stiffness can be not updated when the absolute values of the steering angle, yaw rate and estimated state at a time before are all less than a certain small value. In this simulation study, this certain small value is determined as 0.001 for both front and rear tires. Combining the constraints with RLS, the cornering stiffness of front and rear tires can be estimated well.

6.1. Cornering Stiffness Estimation of Front Tire

For the cornering stiffness of front tire, as seen in Figure 4, a lateral motion trajectory is given to avoid the obstacles in front of vehicle. Corresponding to the required motion trajectory, the changing trend of front steering angle is shown in Figure 5. The lateral force of front tire, which is represented with solid curve, is given in Figure 6. Combining with (13), the regression model, which is given by (17), can be deduced for estimating the cornering stiffness of front tire. RLS is conducted with forgetting factor $\lambda = 0.0995$ and the constraints discussed above. As seen in Figure 5 and Figure 6, front steering angle can be changed at about 1.1s and the lateral force of front tire can

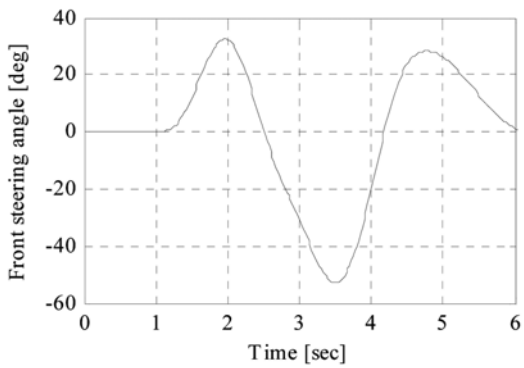

Figure 5. Front steering angle.

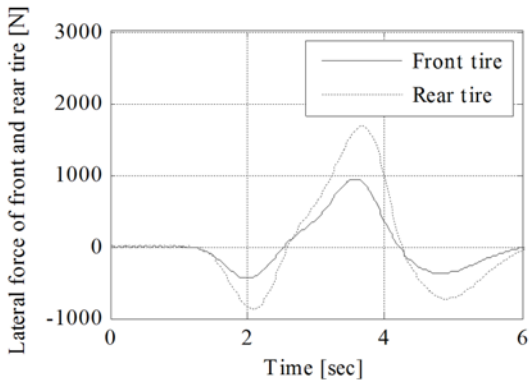

Figure 6. Lateral forces of front and rear tires.

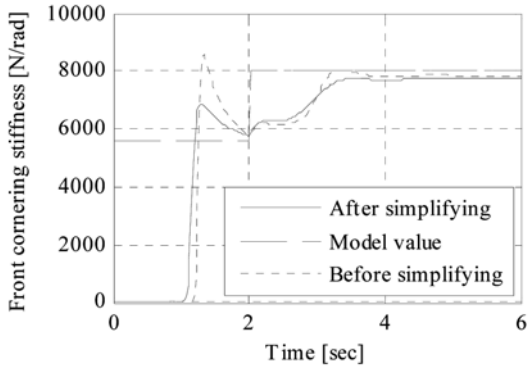

Figure 7. Cornering stiffness estimation of front tire.

be changed at about 1.2s. Therefore, the cornering stiffness of front tire can be estimated after 1s, which is shown in Figure 7. It is assumed that the model value of the cornering stiffness of front tire varies from 5600 N/rad to 8000 N/rad in simulation experiment. As seen in Figure 7, the solid curve represents the estimation value of cornering stiffness of front tire based on (13), and the dotted curve represents the estimation value of cornering stiffness of front tire based on (9) and (12). The solid curve begins to

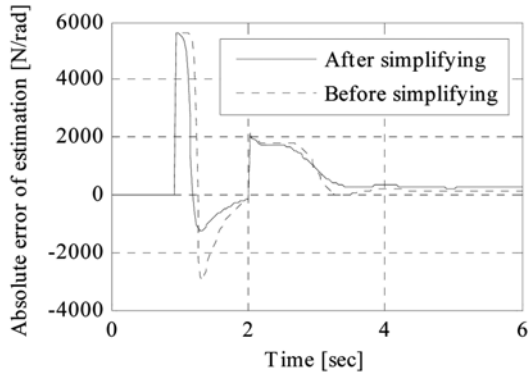

Figure 8. Absolute error of estimation.

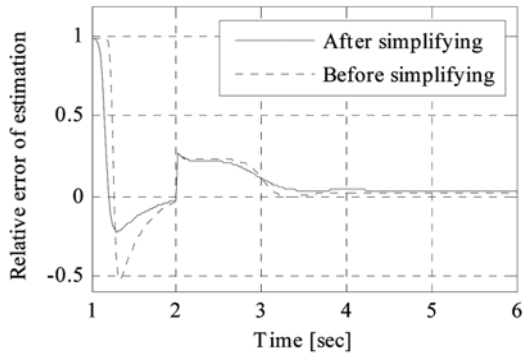

Figure 9. Relative error of estimation.

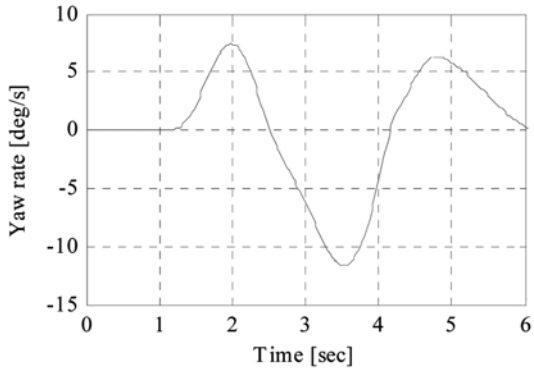

Figure 10. Yaw rate.

estimate at about 1.1s, and the dotted curve begins to estimate at about 1.2s. Therefore, the computation speed based on (13) is faster than that based on (9) and (12). As shown in Figure 8 and Figure 9, respectively, the solid curves represent the absolute error and relative error based on (13), and the dotted curves represent the absolute error and relative error based on (9) and (12), respectively. Although the estimation error based on (13) is a little larger than that based on (9) and (12), the estimated values of cornering stiffness can draw near model values well both before and after simplifying lateral dynamic models. Therefore, the estimated cornering stiffness of front tire based on (13) can be on behalf of road condition for front tire instead of (9) and (12).

6.2. Cornering Stiffness Estimation of Rear Tire

For the cornering stiffness of rear tire, as seen in Figure 10, the changing trend of yaw rate is shown corresponding to the changing of front steering angle. Combining with (14), the regression model, which is given by (17), can be deduced for estimating the cornering stiffness of rear tire. RLS is conducted with forgetting factor $\lambda = 0.0995$ and the constraints discussed above. The longitudinal velocity of vehicle, which is chosen as 90 kph, is required for estimation process. In the same way, as seen in Figure 10 and Figure 6, yaw rate can be changed at about 1.2s and the lateral force of rear tire can be changed at about 1.2s for lateral motion. Therefore, the cornering stiffness of rear tire can be also estimated after 1s, which is shown in Figure 11. It is assumed that the model value of the cornering stiffness of rear tire varies from 18000 N/rad to 8000 N/rad in simulation experiment. As seen in Figure 11, the solid curve represents the estimation value of cornering stiffness of rear tire based on (14), and the dotted curve represents the estimation value of cornering stiffness of rear tire based on (9) and (12). Although the computation speed based on (9) and (12) is faster than that based on (14), the estimation value based on (9) and (12) can not draw near model value well, comparing with that based on (14). As shown in Figure 12 and Figure 13, the solid curve represents the absolute error and relative error based on (14), respectively,

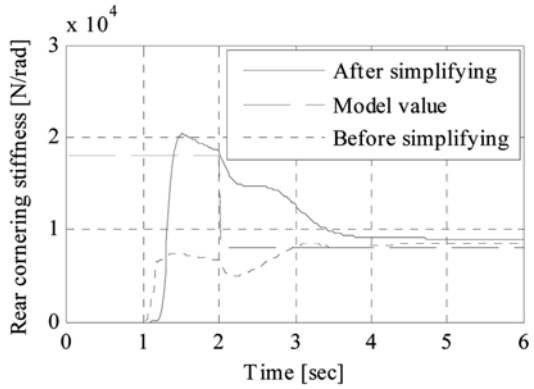

Figure 11. Cornering stiffness estimation of rear tire.

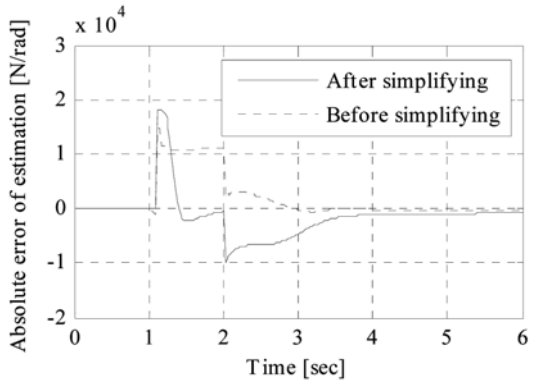

Figure 12. Absolute error of estimation.

and the dotted curve represents the absolute error and relative error based on (9) and (12), respectively. The error curves show that the estimation values of cornering stiffness of rear tire, which is based on (14), can draw near model values well in the whole lateral motion, and that the error based on (9) and (12) is large before 2s. The main reason is that the cornering stiffness of rear tire can be obtained indirectly with two estimation variables. It can be influenced by the estimation error of the cornering stiffness

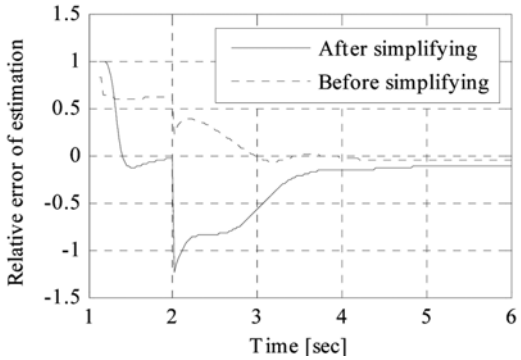

Figure 13. Relative error of estimation.

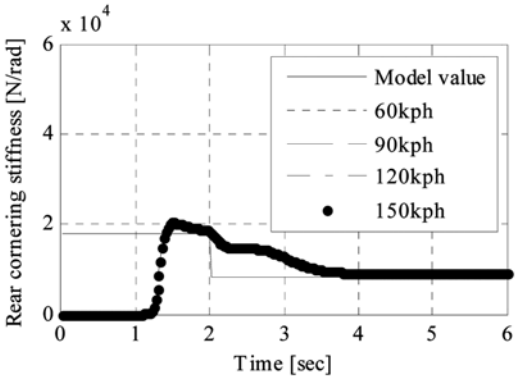

Figure 14. Rear cornering stiffness estimation under different longitudinal velocities.

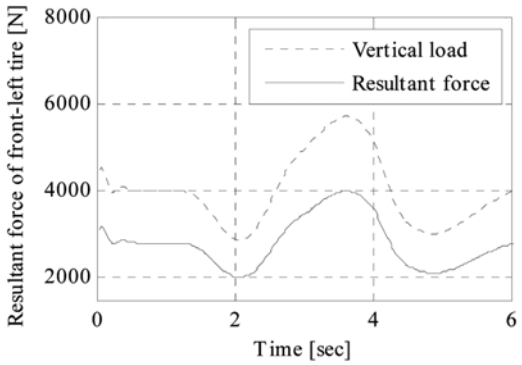

Figure 15. Vertical load of front-left tire.

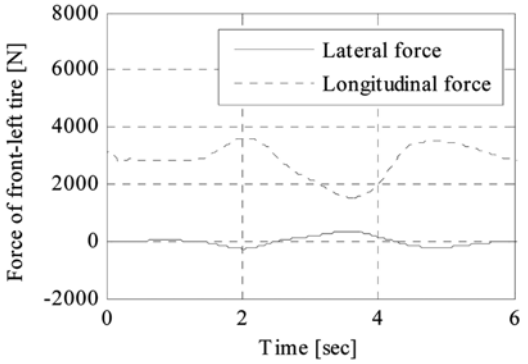

Figure 16. Force of front-left tire.

of front tire based on (9) and (12). But in contrary, it can not be influenced by the estimation error of the cornering stiffness of front tire based on (14). Therefore, the estimated cornering stiffness of rear tire based on (14) can be also on behalf of road condition for rear tire instead of (9) and (12).

In addition, the information on longitudinal velocity is involed in (14) for estimating cornering stiffness of rear tire. It is assumed that model value is invariant. The simulation experiments are implemented under 60 kph, 90 kph, 120 kph, and 150 kph. Contrast estimation curves are shown in Figure 14. They overlap each other during the estimating process of cornering stiffness of rear tire. It can demonstrate that the change of velocity can not influence the effectiveness and reliability of estimator. Therefore, and the estimation of cornering stiffness of rear tire, which is based on simplified lateral dynamic model, can be suitable for different driving conditions.

The simplified lateral dynamic models of front and rear tires are used to construct regression models of RLS without the information on sideslip angle of vehicle, which are so simple that the regression models of RLS are easy to be realized not only in structure, but also in calculation for front and rear tires. What is more important is that the estimation effectiveness of tire cornering stiffness is well in contrast to that before simplifying lateral dynamic models.

6.3. Tire Force Estimation and Distribution

For requirement of simulation study, adhesion coefficient is chosen as 0.7, and the vertical load of each tire can be used as given data. As seen from Figure 15, Figure 17, Figure 19, and Figure 21, the dotted curves represent the vertical load of each tire, which represent the load transfer between the front and rear tires, and between the left and right tires in the whole lateral motion. The solid curves represent the resultant force of each tire, respectively.

The information on lateral force of each tire can be obtained from lateral tire force sensor. The information on longitudinal force of each tire can be estimated from the aforementioned longitudinal tire force observer. According to the constraints of each wheel unit, tire longitudinal forces can be constrained to satisfy the tire forces distribution problem mentioned above. The changing trend of lateral and longitudinal forces of tire and their distribution conditions are shown in Figure 16, Figure 18, Figure 20, and Figure 22 during the whole lateral motion. The information on lateral and longitudinal forces of tire is available to provide the essential information for nonlinear observer of sideslip angle. The lateral tire forces consist of

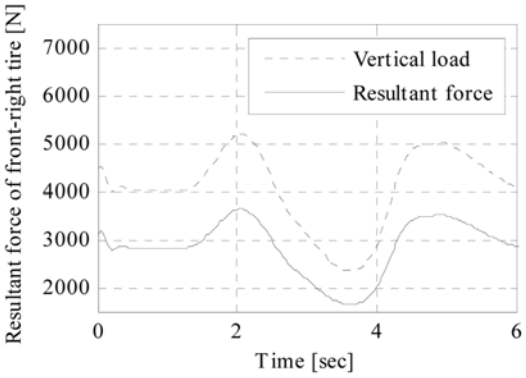

Figure 17. Vertical load of front-right tire.

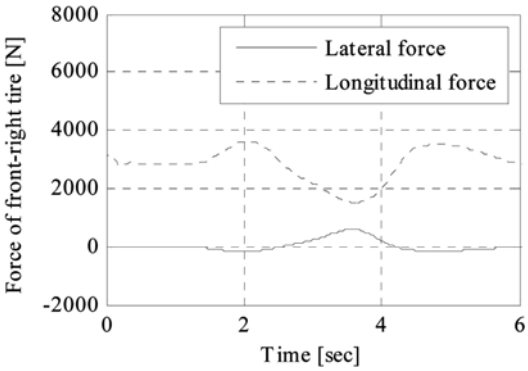

Figure 18. Force of front-right tire.

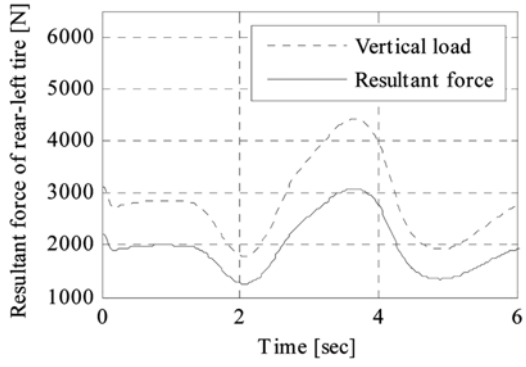

Figure 19. Vertical load of rear-left tire.

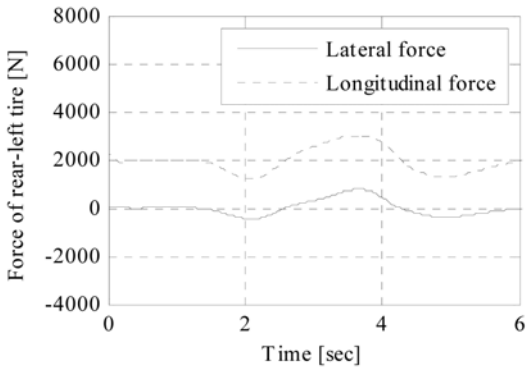

Figure 20. Force of rear-left tire.

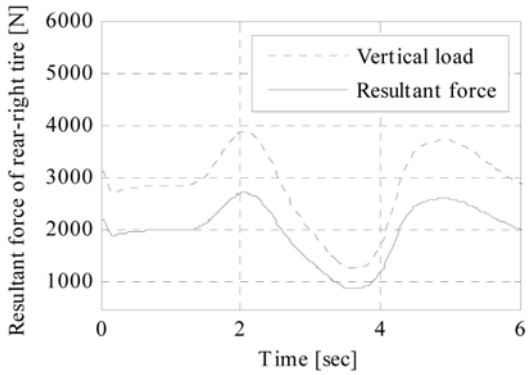

Figure 21. Vertical load of rear-right tire.

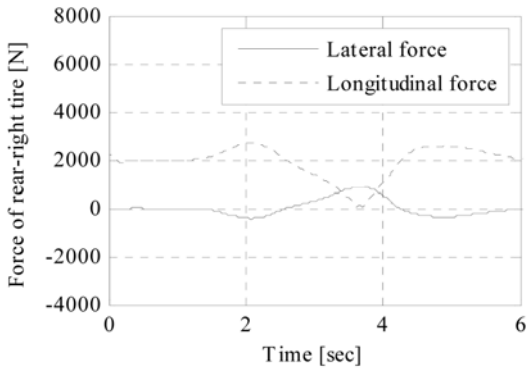

Figure 22. Force of rear-right tire.

the state vector and measurement vector of nonlinear observer of sideslip angle, and the longitudinal tire forces consist of the input vector of nonlinear observer of sideslip angle. They can be also employed to participate in controlling attitude of vehicle to keep the desire trajectory, besides vehicle parameters estimation.

6.4. Sideslip Angle Estimation

Combining the discretization of nonlinear observer of sideslip angle designed above with DD1-filter, sideslip angle is estimated with the information on tire cornering stiffness. In the whole lateral motion shown in Figure 4, the information on front steering angle, yaw rate, front left driving force, front right driving force, rear left driving force, rear right driving force, front lateral tire force, and rear lateral tire force, which are shown in Figure 5, Figure 10, Figure 16, Figure 18, Figure 20, and Figure 22, respectively, is used in nonlinear observer of sideslip angle.

Besides that, the initial covariance P_0, covariance of process noise Q, covariance of measurement noise R, and initial state x_0 are given as the initialization parameters of DD1-filter in simulations as follows:

$$P_0 = diag([1,1,1,1,1,1]);\ Q = diag\left(\left[\frac{1}{2}, \frac{1}{2}, \frac{1}{2}, \frac{1}{2}, \frac{1}{2}, \frac{1}{2}\right]\right);$$

$$R = diag([4,\ 4,\ 4,\ 4,\ 4)];\ x_0 = [0,\ 0,\ 0,\ 0,\ 12000,\ 28000)]^T.$$

With the initial covariance and state, DD1-filter can be implemented easily, and the sideslip angle of vehicle can be estimated. As seen in Figure 23, the estimation results of DD1-filter are represented by dotted curve, and the estimated value of sideslip angle is easy to be disturbed. Therefore, a first-order low-pass filter, which is used to filter out interference, is employed as follows:

$$y(k) = \frac{KT_c}{T+T_c}u(k) + \frac{T}{T+T_c}y(k-1) \tag{51}$$

where, K is proportionality coefficient, $K=1$; T is time constant, $T=50.5$s; T_c is sampling time, $T_c=30.5$s. The filtered results are represented by solid curve in Figure 23, and the filtering effect is batter than that before filtering. In terms of the vehicle motion trajectory, the range of sideslip angle is between −2.1285 and 4.1382° in the whole lateral motion. The compututation speed of estimator is fast, and sideslip angle estimator is stable in estimation process. The simulation results demonstrate that sideslip angle estimation is effective, reliable, and accurate. The estimation error of sideslip angle of vehicle is shown in Figure 24. The error range represented by dotted curve is between −0.3162° and −0.0012°. The error range represented by solid curve is between −0.117 and 0.00°. The estimation error of sideslip angle with DD1 and a first-order low-pass filter is smaller than that with DD1-filter. By utilizing the information on tire cornering stiffness estimated with simplified lateral dynamic models, accurate and reliable state estimation of sideslip angle can be realized.

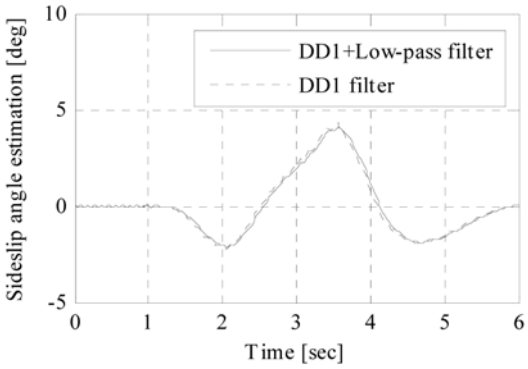

Figure 23. Sideslip angle estimation.

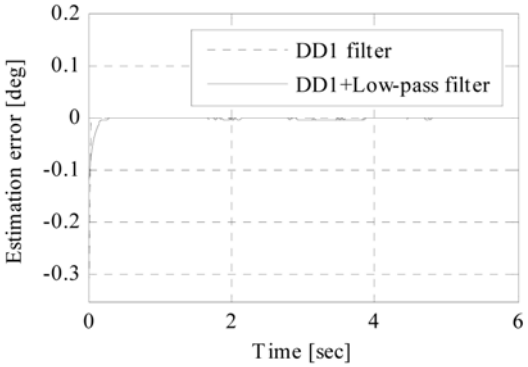

Figure 24. Estimation error of sideslip angle.

7. CONCLUSION

This paper has presented the simplified lateral dynamic models of front and rear tires about tire cornering stiffness, which are employed to construct the regression models used in RLS with forgetting factors and constraints. With the estimated information on tire cornering stiffness, a nonlinear observer of sideslip angle for FIWMD-EVs can be designed, and sideslip angle can be also estimated through DD1-filter and a first-order low-pass filter.

For tire cornering stiffness estimation, they can be estimated with neither the information on sideslip angle, nor interactive influences in estimating process. Consequently, the tire cornering stiffness of front and rear tires can be estimated independently with lateral tire force information. Furthermore, the estimation effectiveness of cornering stiffness of rear tire is not influenced on longitudinal velocity of vehicle, although the information on longitudinal velocity of vehicle is required in the simplified lateral dynamic model of cornering stiffness of rear tire. The reliability, feasibility, effectiveness, and practicality of the simplified lateral dynamic models are verified by comparing with the features before simplifying lateral dynamic models in simulations. Computational burden can be reduced and computation speed can be improved due to the simplified lateral dynamic models. Therefore, the estimation of tire cornering stiffness after simplifying lateral dynamic models can be on behalf of road condition precisely instead of the estimation of tire cornering stiffness before simplifying lateral dynamic models.

For sideslip angle estimation, with the information on tire cornering stiffness based on the simplified lateral dynamic models of front and rear tires, a nonlinear observer of sideslip angle can be designed conveniently for FIWMD-EVs. Based on the designed nonlinear observer of sideslip angle, sideslip angle is estimated making use of a DD1-filter and a first-order low-pass filter in the whole lateral motion. The nonlinear observer of sideslip angle is simple in structure, and easy to implement.

In addition, on the one hand, tire cornering stiffness can be used to estimate sideslip angle through the design of the nonlinear observer of sideslip angle; on the other hand, tire cornering stiffness can be benefit to the research and design

of lateral stability control system, such as the lateral adaptive controller, which can make vehicle adapt to the different road conditions, the direct yaw moment controller, which can control the attitude of vehicle motion. This work is left for future studies and improved more.

REFERENCES

Abe, M. and Manning, W. (2009). *Vehicle Handling Dynamics Theory and Application*. Elsevier.

Anderson, R. and Bevly, D. M. (2005). Estimation of tire cornering stiffness using GPS to improve model based estimation of vehicle states. *Proc. IEEE Intelligent Vehicles Symp.*, 801–806.

Aparicio, F., Paez, J., Moreno, F., Jimenez, F. and Lopez, A. (2005). Discussion of a new adaptive speed control system incorporating the geometric characteristics of the road. *Int. J. Veh. Auton. Sys*. **3**, **1**, 47–64.

Arndt, C., Karidas, J. and Busch, R. (2004). Design and validation of a vehicle state estimator. *Proc. 7th AVEC*, 41–45.

Baffet, G., Charara, A. and Lechner, D. (2007). Experimental evaluation of sliding mode observer for tire-road forces and an extended kalman filter for vehicle sideslip angle. *Proc. 46th IEEE Conf. Decision and Control*, 3877–3882.

Baffet, G., Stephant, J. and Charara, A. (2006). Vehicle sideslip angle and lateral tire-force estimations in standard and critical driving situations: Simulations and experiments. *Proc. 8th Int. Symp. AVEC*, 41–45.

Cheli, F., Sabbioni, E., Pesce, M. and Melzi, S. (2007). A methodology for vehicle slip angle identification: comparison with experiment data. *Vehicle System Dynamics* **45**, **6**, 549–563.

Doumiati, M., Victorino, A. C., Charara, A. and Lechner, D. (2011). Onboard real-time estimation of vehicle lateral tire-road forces and sideslip angle. *IEEE Trans. Mechatronics* **16**, **4**, 601–614.

Fredriksson, J., Andresson, J. and Laine, L. (2004). Wheel force distribution for improved handling in a hybrid electric vehicle using nonlinear control. *43rd IEEE Conf. Decision and Control*, 4081–4086.

Fujimoto, H., Takahashi, N. and Tsumasaka, A. (2006). Motion control of electric vehicle based on cornering stiffness estimation with yaw moment observer. *Proc. IEEE Int. Workshop on Advanced Motion Control*, 206–211.

Fujimoto, H., Tsumasaka, A. and Noguchi, T. (2005). Direct yaw-moment control of electric vehicle based on cornering stiffness estimation. *Proc. IEEE IECON*, 2626–2631.

Geng, C., Mostefai, L., Denai, M. and Hori, Y. (2009). Direct yaw-moment control of an in-wheel-motored electric vehicle based on body slip angle fuzzy observer. *IEEE Trans. Ind. Electron.* **56**, **5**, 1411–1419.

Geng, C., Uchida, T. and Hori, Y. (2007). Body slip angle estimation and control for electric vehicle with in-wheel motors. *Proc.33rd IEEE IECON*, 351–355.

Grip, H. F., Imsland, L., Johansen, T. A., Kalkkuhl, J. C. and Suissa, A. (2009). Vehicle sideslip estimation: Design, implementation and experimental validation. *IEEE Control Syst. Mag.* **29**, **5**, 36–52.

Han, S. and Huh, K. (2011). Monitoring system design for lateral vehicle motion. *IEEE Trans. Veh. Technol.* **60**, **4**, 1394–1403.

Holweg, E. (2008). Vehicle dynamics and safety. *High Tech Automotive Systems*. Subsidieregelingen.

Huh, K. and Kim, J. (2001). Active steering control based on the estimated tire forces. *Trans. ASME, J. Dyn. Syst. Meas. Control* **123**, **3**, 505–511.

Imsland, L., Johansen, T. A., Fossen, T. I., Grip, H. F., Kalkkuhl, J. C. and Suissa, A. (2006). Vehicle velocity estimation using nonlinear observer. *Automatic* **42**, **12**, 2091–2103.

Jazar, R. (2008). *Vehicle Dynamics: Theory and Applications*. Springer. New York.

Ko, S. Y., Ko, J. W., Lee, S. M., Cheon, J. S. and Kim, H. S. (2014). Vehicle velocity estimation using effective inertia for an in-wheel electric vehicle. *Int. J. Automotive Technology* **15**, **5**, 815–821.

Lechner, D. (2008). Embedded laboratory for vehicle dynamic measurements. *9th Int. Symp. Adv. Veh. Control*.

Leeuween, B. V. and Zuurbier, J. (2007). Vehicle state estimation based on load sensing. *Vehicle Dynamics Expo*.

Lian, Y. F., Tian, Y. T., Hu, L. L. and Yin, C. (2012). Development of identification of tire-road friction conditions. *12th Int. Conf. Control, Automation, Robotics & Vision*, 1812–1817.

Nam, K., Fujimoto, H. and Hori, Y. (2012). Lateral stability control of in-wheel-motor-driven electric vehicle based on sideslip angle estimation using lateral tire force sensors. *IEEE Trans. Veh. Technol.* **61**, **5**, 1972–1985.

Nguyen, B. M., Nam, K., Fujimoto, H. and Hori, Y. (2011). Proposal of cornering stiffness estimation without vehicle sideslip angle using lateral force sensor. *IEEJ Technical Meeting Record* **IIC-11-140**, 37–42.

Nishio, A., Tozu, K., Yamaguchi, H., Asano, K. and Amano, Y. (2001). Development of vehicle stability control system based on vehicle sideslip angle estimation. *SAE Paper No*. 2001-01-0137.

Norgaard, M., Poulsen, N. K. and Ravn, O. (2000). New Developments in State Estimation for Nonlinear Systems. *Automatica*, 1627–1638.

Piyabongkarn, D., Rajamani, R., Grogg, J. A. and Lew, J. Y. (2009). Development and experimental evaluation of a slip angle estimator for vehicle stability control. *IEEE Trans. Contrl Syst. Technol*. **17**, **1**, 78–88.

Rajamani, R. (2005). *Vehicle Dynamics and Control*. Springer. New York.

Rajamani, R., Phanomchoeng, G., Piyabongkarn, D. and

Lew, J. Y. (2012). Algorithms for real-time estimation of individual wheel tire-road friction coefficients. *IEEE Trans. Mechatronics* **17**, **6**, 1183–1195.

Sado, H., Sakai, S. and Hori, Y. (1999). Road condition estimation for traction control in electric vehicle. *Proc. IEEE. ISIE*, 973–978.

Shino, M., Yoshitake, H., Hiramatsu, M., Sunda, T. and Kamata, M. (2014). Deviated state detection method in driving around curves based on naturalistic driving behavior database for driver assistance systems. *Int. J. Automotive Technology* **15**, **5**, 749–755.

Sienel, W. (1997). Estimation for tire cornering stiffness and its application to active car steering. *36th Conf. Decision & Control*, 4744–4749.

Sierra, C., Tseng, E., Jain, A. and Peng, H. (2006). Cornering stiffness estimation based on vehicle lateral dynamics. *Vehicle System Dynamics*, **44**, 24–38.

Tunonen, A. J. (2008). Optical position detection to measure tyre carcass deflection. *Vehicle System Dynamics* **46**, **6**, 471–481.

Wenzel, T. A., Burnham, K. J., Blundell, M. and Williams, R. (2006). Motion dual extended Kalman filter for vehicle state and parameter estimation. *Vehicle System Dynamics* **44**, **2**, 153–171.